J. Fluid Mech. (1969), *vol.* 35, *part* 2, *pp.* 337–352
Printed in Great Britain

Change in wave-form and mean flow associated with wavelength variations in rotating Couette flow. Part 1

By H. A. SNYDER†
Woods Hole Oceanographic Institution, Woods Hole,
Massachusetts 02543

(Received 24 January 1968 and in revised form 19 July 1968)

When rotating Couette flow becomes unstable a periodic vortex structure is formed. For the wide-gap case, this flow is steady for a rather large range of the Taylor number above onset. In the region of finite amplitude instability the wave-numbers of the periodic structure are not unique. It is shown empirically that the non-uniqueness is not an end effect but a bonafide property of the flow and that the wave-form is a unique function of the wavelength. Data is presented to demonstrate the interval over which the wave-numbers can be varied when the parameters of the system are fixed. The large effect on the wave-form of small changes in the wavelength is also illustrated. These conclusions are based on extensive measurements of the azimuthal drift velocity for a particular mode of secondary flow.

1. Introduction

An interesting feature of non-linear mechanics is that a steady-state solution to the equations of motion may under certain circumstances be determined not only by the steady-state boundary conditions but also by the past history of the system. This occurs when there is a manifold of steady solutions for each point in parameter space and the selection from this set is determined by the initial conditions or past history of the boundary conditions. The problems of supercritical cellular flows fall into this category.

At the present time general methods for picking out a particular solution to a non-linear problem from the allowed set are not known. But currently there is a great deal of activity aimed at solving this problem. Most of the work is theoretical; the reader can find many details and references to current articles in, for example, Ekhaus (1965) and Segel (1966). Very little experimental work on the selection problem has appeared in the literature. The author has reviewed the available data and has presented some original measurements in a previous article, Snyder (1968*a*). Quite a bit remains to be learned about this subject before we can predict the behaviour of the simplest cases. The present research is devoted to establishing certain results that may be used as a guide in the very complex theoretical investigations.

† On leave from Department of Physics, Brown University.

Of those problems which exhibit the non-uniqueness under discussion perhaps the easiest case to treat both theoretically and experimentally is that of rotating Couette flow. There is no loss of generality in choosing this flow over others since the non-linear term in the governing equation is the same for all the forms of cellular flow and it is the non-linear term which accounts for the interesting effects.

It is well known that in the supercritical region the flow between concentric rotating cylinders consists of cellular vortices. If the axis of rotation is vertical, the axes of the vortices lie in a horizontal plane. They are vortex rings stacked one upon another; adjacent cells have opposite sense of rotation. The flow is therefore periodic in the axial direction (singly periodic); a pair of vortices constitutes a wavelength. It is also possible for the wave-form to be periodic in the azimuthal direction in addition to its axial periodicity (doubly periodic). In the latter case the wave-form, which is no longer rotationally symmetric, drifts relative to the containing cylinders and has an angular frequency in the laboratory frame which we will designate $\tilde{\omega}$. Pictures of both singly and doubly periodic cells may be found in an article by Coles (1965).

The non-uniqueness of rotating Couette flow is evident in the wavelength of the disturbance in the axial direction λ, as well as in the aximuthal wave-number m, if the flow is doubly periodic. For a fixed geometry and dimensions of the apparatus, and for fixed rates of rotation of the cylinders, i.e. fixed boundary conditions, it is possible to have a range of different wavelengths in the axial direction and several different wave-numbers in the azimuthal direction. We will be interested in this paper in how the different properties of the wave-form are influenced by changes in the wavelength when the boundary conditions are held fixed. In particular we will measure the drift velocity at fixed boundary conditions; this data will be used to show that rather small changes in the wavelength at constant conditions cause the secondary flow to be strongly modified.

The fact that the wavelength of the disturbance in Couette flow is not a unique function of the Taylor number, the clearance ratio, and the angular velocity ratio of the cylinders (the dimensionless governing parameters of the steady-state equation) was demonstrated in an important piece of research by Coles (1965). Let us designate: the Taylor number by $T = (\Omega_1 d^2/\nu)^2$, where Ω_1 is the angular velocity of the inner cylinder, d is the gap width and ν is the kinematic viscosity; $Re_1 = (T)^{\frac{1}{2}}$; the clearance ratio by $\eta = R_1/R_2$, where $R_2 > R_1$ are the radii of the cylinders; the angular velocity ratio by $\mu = \Omega_2/\Omega_1$; and the length to gap ratio by $\gamma = L/d$, where L is the height of the fluid column. Coles, using an apparatus with $\eta = 0{\cdot}875$ and γ fixed at 27·9, has shown that with $\mu = 0$ and Re_1 somewhat above the onset value, the secondary wave-form is doubly periodic in the axial z, and in the azimuthal θ directions, i.e. each variable has a dependence proportional to $\exp i(kz + m\theta - \omega t)$, where k is the axial wave-number or $2\pi/\lambda$. It is obvious that m is an integer and that the number of half wavelengths in L is also an integer, call it N. As Coles varied Re_1 he found that various modes characterized by $(2N, m)$ occurred, and that the range for the different $(2N, m)$ overlapped. When the wave-form is non-unique the past history of the apparatus determines the values $(2N, m)$.

In an earlier experiment Hagerty (1946) used an apparatus in which the level of the fluid could be raised or lowered while the cylinders were rotating. He found that when L was changed while Re_1 was above its critical value, λ the wavelength, could be decreased by draining or increased by adding fluid. The value of N stayed constant over a rather large range of L for fixed Re_1. There was an overlap in the plot of N *vs.* L for adjacent integers N. In Hagerty's experiments the length to gap ratio $\gamma \approx 6$ so that end effects were important in determining the wave-form.

There has been speculation by several different workers in this field on Coles' results concerning non-uniqueness, Segel (1966, p. 191), Davey, DiPrima & Stuart (1968, p. 19). It is suggested that the effect arises from the end conditions and that in a sufficiently long apparatus the effect would not appear. One of the motivations for the present paper is to test this hypothesis. The results we will present show that the lack of uniqueness is not an end effect.

It also occurred to the author that the properties of the wave-form should be a function of the wavelength λ, and that N is an irrelevant parameter. In the work on end effects it is shown that $\lambda \neq 2L/N$ because the cell of secondary flow at each end of the apparatus is not a Taylor cell; its length may deviate from that of the intervening Taylor vortices by as much as a factor of two. We will prove in what follows that when two different values of N give the same λ, then, the wave-forms are identical.

The third purpose of this research is to see how large the relative difference in the observable properties of the wave-form might be when the wavelength is varied by about 20 or 30 %. There are several properties that can be measured: (*a*) the torque on the inner cylinder, (*b*) the circulation and harmonic generation in the secondary flow, or (*c*) the drift velocity, in the case of doubly periodic wave-forms. We have made measurements on all three observables but will report only the results of case (*c*) in this paper.

The measurements of the drift velocity are reproducible to better than 1 % from run to run and day to day; they are easy to take and interpret. Furthermore, the drift velocity results are sufficient to answer the purposes of the research as set forth above. At present, the data on cases (*a*) and (*b*) show relative changes with λ having a maximum of about 30 % with a scatter of ± 10 %. We are presently trying to reduce the scatter in the data of cases (*a*) and (*b*), and hope to present the results as part II of this paper shortly.

2. Methods and equipment

The method combines features of both Coles's (1965) and Hagerty's (1946) experiments. A doubly periodic mode with $m = 2$ is chosen for study. L, the length of the fluid column, is varied as in Hagerty's investigation and Re_1 is varied as Coles has done. The angular frequency of the wave-form (the drift velocity) $\omega/m = \tilde{\omega}$, or more frequently ω, is measured. The results form a three entry table for $\tilde{\omega}$ or ω in terms of Re_1, Re_2 and λ; these are the four variables that are measured. More details of the procedure will be presented later.

2.1. *Equipment*

The apparatus is described in previous publications: see Snyder & Karlsson (1964), Lambert, Snyder & Karlsson (1965) and Snyder (1968*b*) for most of the details. The value of η is selected to be $\frac{1}{2}$ because other experiments have shown that the mode $m = 2$ has the largest area in parameter space for $\eta \approx \frac{1}{2}$. For the present data $R_1 = d = 3{\cdot}140$ cm. The maximum value of L is 95 cm. The base of the annular space between the cylinders rotates with the inner cylinder, and the upper surface of the fluid column is a free surface. Thermal baths inside the inner cylinder and outside the outer cylinder maintain the annular region isothermal to about $\pm 0{\cdot}005\,^{\circ}$C.

The path lines of the flow are made visible by aluminium flakes suspended in the aqueous solution of glycerol used as the working fluid. A plane through the axis of rotation about 2 mm in thickness is lighted with parallel light. The lighted plane is observed at normal incidence by a photocell. The output of the photocell has the period $2\pi/\omega$. This signal is recorded and ω can be read off the recorder trace.

In calculating Re_1 and Re_2 it is necessary to know Ω_1, Ω_2 and ν. The two variables Ω_1 and Ω_2 are measured by magnetic pick-ups controlling electronic counters. The speed of the drive motors is constant to within the variations of the line frequency, or about $\pm 0{\cdot}2$ %. The speed can be measured to about the same accuracy.

A Cannon–Fenske viscometer is used to find ν at the beginning and end of each set of runs. An accuracy of 1 % is generally claimed by the manufacturers for this instrument. A high viscoscity solution, usually about 1·0 cm^2/sec, is used to reduce the transient equalization time of the wavelengths. Although this time for a singly periodic cell has been shown in a previous publication, Snyder (1968*a*), to be about $L^2/6\nu$, the vertical motion of the doubly periodic cell reduces the time to about $L^2/25\nu$ or about 4 min in these experiments.

The wavelength of the secondary flow is observed with a cathetometer focused on the lighted axial plane. At normal incidence the instrument is both sensitive and accurate to 0·1 mm. Since $\lambda \approx 5$ cm, the measurements of the wavelength are good to better than 1 %.

2.2. *Procedure*

Two different types of experiments were carried out. In the first, Re_1 and Re_2 are held fixed. The apparatus is started in such a manner that the number of secondary cells N has a desired value (see Snyder 1968*a* for the procedure for setting up a particular number of cells). The level of the fluid L is set at a desired height. The system is allowed to run for the transient equalization time—about $L^2/25\nu$, i.e. 4 min. Then, λ the wavelength and ω the angular frequency of the wave-form are measured. The level is increased or decreased to a new value and the process is repeated.

The result is a curve of ω *vs.* λ for fixed Re_1 and Re_2. When L reaches a critical value, there is a transition to a new number of cells $N \pm 1$; this transition limits the extent of the curve. If Re_1 and Re_2 are not close to the edge of the region

where $m = 2$ in the Taylor number plane there are no transitions to a new value of m. It is important in taking the data that after each change of conditions, the system must run for the transient equalization time before a reading is made.

The second type of data is a plot of ω *vs.* Re_2 for fixed λ and Re_1. Again the apparatus is started in a way which will give a desired value of N, the number of cells. Then, λ and ω are measured. Re_2 is changed to a new value and fluid is added or subtracted to keep λ constant; recall that the length of the cells at the ends may be a function of Re_2. After the necessary waiting time the new value of ω is measured. This process continues until there is a transition to $N \pm 1$ or to a new value of m.

Because of hysteresis in the transitions $N \to N \pm 1$ and $m \to m'$, the precise path followed in parameter space when taking the data must be specified. Figure 1 illustrates where the various modes of secondary flow are found when

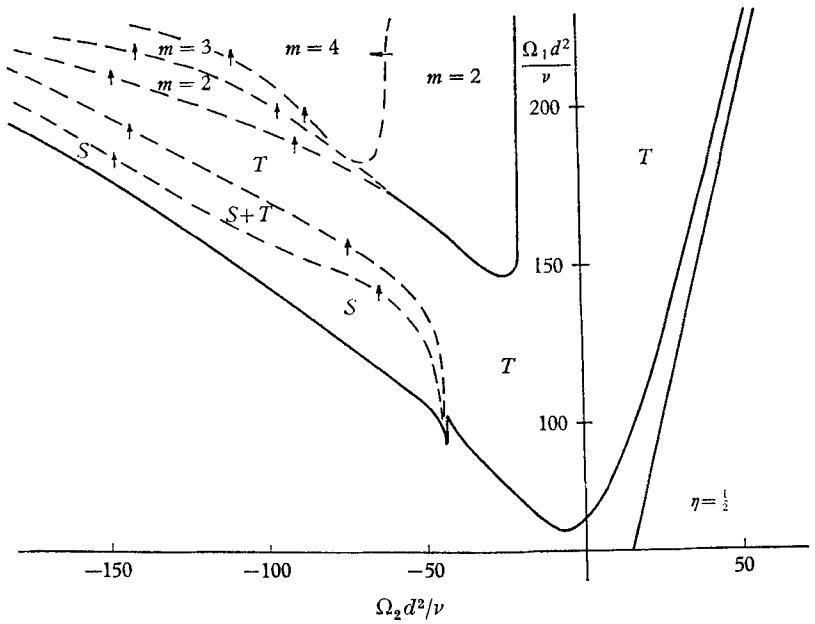

FIGURE 1. The wave-form diagram for an apparatus with $R_2 = 2R_1$. T, Taylor vortices; S, spirals; $m = 2, 3, 4$, doubly periodic cells with aximuthal wave-number m. Hysteresis is indicated by dotted lines.

$\eta = \frac{1}{2}$. Solid lines indicate that no hysteresis occurs in traversing the line in any direction. When there is hysteresis, the line is dotted and the arrow points in the direction of traverse which results in the line indicated. All lines show the maximum extent of the region of more complicated wave-form for all attainable values of λ. In the figure, T means a simple Taylor vortex, S is a spiral, $S + T$ is a mixture, and m indicates a doubly periodic wave-form with the appropriate value of m. Note that only singly periodic wave-forms occur to the right of $Re_2 = -15$. We will be concerned only with the mode $m = 2$. All step by step

passes across this region will be at constant Re_1, i.e. a horizontal line in the figure, and from right to left, i.e. toward increasingly negative values of Re_2. For fixed Re_1 and Re_2 the course is toward shallower depths, decreasing L.

3. Results

3.1. *The wave-form*

The wave-form which occurs in the area of figure 1 designated as $m = 2$ is a complicated mixture of linear normal modes. The predominant mode has axial wave-number k and azimuthal wave-number $m = 2$. But there is a large amount of harmonic generation on the wave-form.

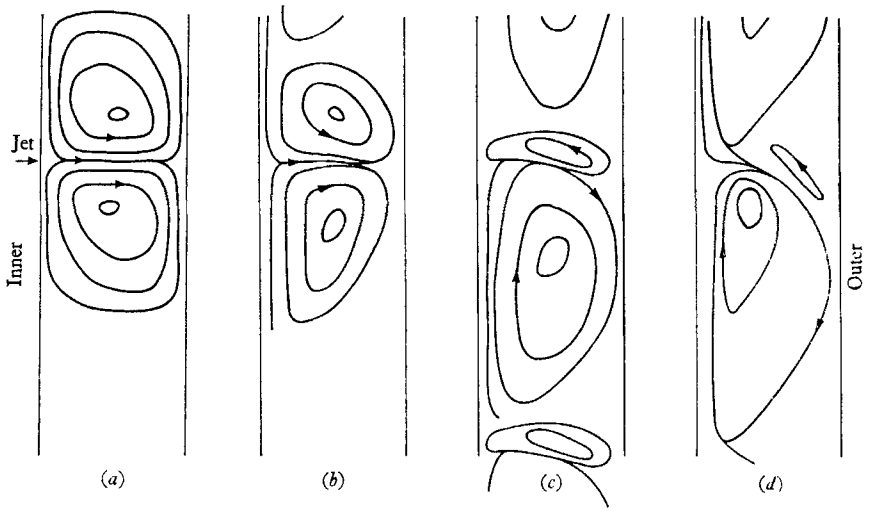

FIGURE 2. A quarter period of the wave-form whose largest component is $m = 2$.

Figure 2 contains four sketches of the streaklines and represents $\frac{1}{4}$ the cycle of the wave-form. It represents what one sees in the lighted plane as the wave-form drifts by. The sequence starts with streaklines that are symmetric about a strong out-going jet (from inner to outer cylinder). There is a weak return flow. The out-going jet swings down slightly as in (*b*), and the lower cell of the pair enlarges at the expense of the neighbouring upper cell. As the axis of the out-going jet turns down farther, as in (*c*) and (*d*), the lower cell continues to grow while the upper cell diminishes until it is hardly visible. Then, the sequence reverses so that we have (*d*), (*c*), (*b*), and finally a symmetric shape. Next, the outgoing jet turns upward and the sequence is the mirror image of figure 2. Coles (1965) has photographed a wave-form that is qualitative similar; see his plates 2, 3 and 4.

The relative change in the size of a cell as it progresses from the symmetrical state to the case shown in figure 2(*d*) depends upon Re_1. The lowest value at which the $m = 2$ mode appears is $Re_1 = 145$ (see figure 1). Near onset of the mode, the amplitude of oscillation of the cell size is very small; but when $Re_1 \approx 160$ the wave-form looks like figure 2 for all attainable values of Re_2. There is very

little change in the appearance of the streaklines as Re_1 and Re_2 are varied throughout the range of the mode, provided $Re_1 > 160$.

It is notable that the components of harmonic generation in both the axial and azimuthal directions are in phase with the fundamental. We pointed out earlier (Snyder & Lambert 1966) that for simple Taylor cells, the components generated by harmonic generation on the axial periodicity have the same phase as the fundamental—this is the origin of the strong out-going jet. Here, the jet formation is evident, but even more striking is the effect of the harmonic content of the azimuthal mode. The wave-form viewed with front lighting (not as we described earlier but as Coles (1965) has used) so that an entire period of the secondary flow is visible, shows that the cell boundaries defined by the out-going jet as it impinges on the outer cylinder have a saw-tooth shape. Two other features of interest are: (*a*) that during a period of oscillation the origin of the out-going jet, at the inner cylinder, does not move by more than 2 or 3 % of the amplitude of the downstream end, i.e. it is fixed in space, and (*b*) that all pairs of cells throughout the length of the fluid column are in phase.

The transition from mode $m = 2$ to the Taylor vortices (see figure 1) is simple; the amplitude of oscillation merely decreases until no θ-dependence is observable. We should note at this point that an outer row of vortices, sometimes predicted to occur beyond the nodal radius at which the tangential velocity is zero, has not been observed either in the T or $m = 2$ regions. The change over from $m = 2$ to $m > 2$ or from N to $N \pm 1$ is preceded by a precurser of the transition; the pairs of cells lose their phase coherence. The column breaks up into several groups of cells which are coherent among themselves but differ in phase with other groups. There is a region of non-conformity between the groups. This phenomenon occurs in a band of width about 5 Reynolds numbers along the transition boundary.

3.2. *The wavelength vs. length to gap ratio as a significant variable*

For cylinders of infinite length the onset of instability for a Newtonian fluid is completely specified by Re_1, Re_2 and η the radius ratio. For real cylinders one would expect the parameter $L/d = \gamma$ to enter. In the finite amplitude region Coles (1965) finds that the number of cells N must also be treated as an independent variable. Some have questioned whether Coles's results still hold if the length to gap ratio is made very large; see Segel's (1966) review. As described above we investigated this problem by taking sets of data such as figure 3.

The frequency of the wave-form observed in the laboratory frame f, i.e. $f = \omega/2\pi$, is plotted in dimensionless form against the equivalent length measured in gap widths. Here, the equivalent length is the length of the fluid column minus the height of the boundary cells at both ends of the column. The number associated with each curve is the number of Taylor cell pairs, i.e. the number of wavelengths of the disturbance, observed. The operating point for all the data on the curve has $Re_1 = 250$, $Re_2 = -55$. This point is located well away from the boundaries of the region $m = 2$ shown in figure 1. If the wavelength is calculated for successive curves with fixed values of fd^2/ν the wavelength is always the same. For example, when $fd^2/\nu = 0$, the dimensionless wavelength λ/d is 1·76 for all the

curves in the figure, and when $df^2/\nu = 2$, $\lambda/d = 1{\cdot}52$ for each curve. Thus, there is a unique relation between λ/d and fd^2/ν; L/d or γ does not affect the results when there are more than 10 cells. However, when the value of the equivalent gap widths gets less than 10, then end effects are important and λ/d depends not only on μ but also on γ.

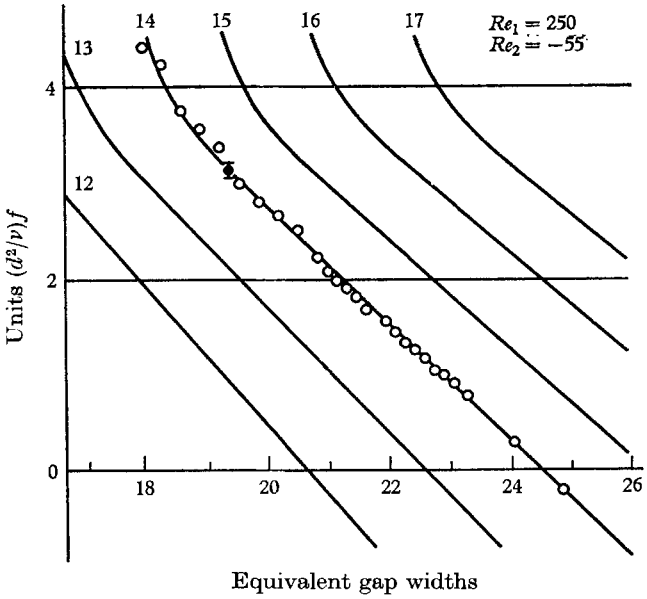

FIGURE 3. The dimensionless frequency of the wave form $m = 2$ *vs.* the height of the fluid column L. The abscissa is L in units of gap width. The numbers on each curve denote the number of cells in the column.

Figure 3 is only one example of a number of data sets that have been taken for various combinations (Re_1, Re_2). All the plots similar to figure 3 have the common property that the curves for different N are nearly parallel, although the straightness of the lines, as in the example, is not a general characteristic. Another common feature of this data is that λ/d reaches a saturation value as it decreases; a transition to $N+1$ or $N+2$ occurs if an attempt is made to reduce λ/d below this value. The scatter of the data on the curve marked '14' is indicative of all the drift velocity measurements reported here.

3.3. *Drift velocity vs. wavelength*

The remaining curves are reduced from sets of data such as figure 4. The dimensionless angular drift velocity is measured as a function of Re_1 and Re_2 for fixed values of λ/d. The range of Re_1 which has been studied is from 160 to 350. The lower limit is set by the decrease of the amplitude of oscillation as Re_1 decreases; while at the upper limit, the cells at the ends of the apparatus become unstable and disturbances are propagated along the column of cells. The value of Re_1 is held constant while Re_2 is increased toward larger negative values. The standard values of Re_1 which are observed are indicated by numbers on the curves.

From data such as that shown in figure 4, the figures 5 to 10 have been

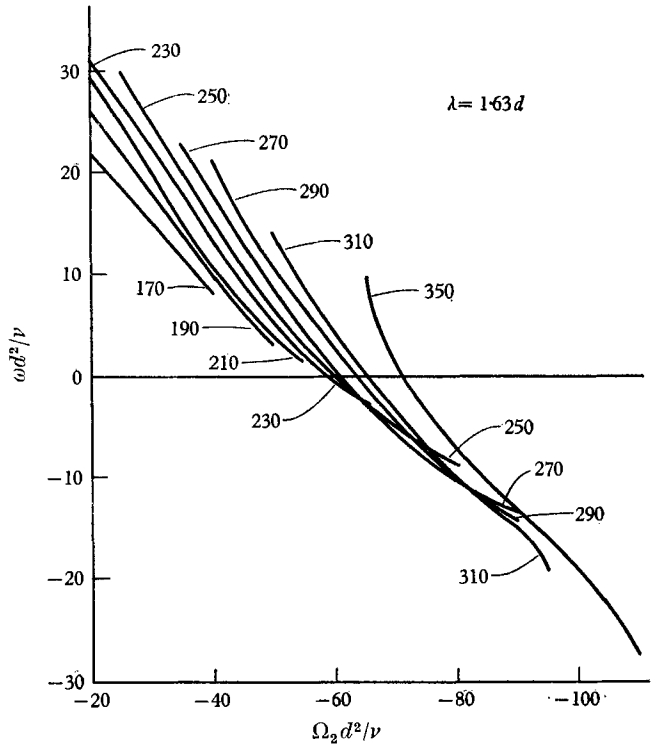

FIGURE 4. The dimensionless angular velocity of the wave-form *vs.* the Reynolds number of the outer cylinder for fixed values of the Reynolds number of the inner cylinder. The wavelength is maintained at 1·63 times the gap width.

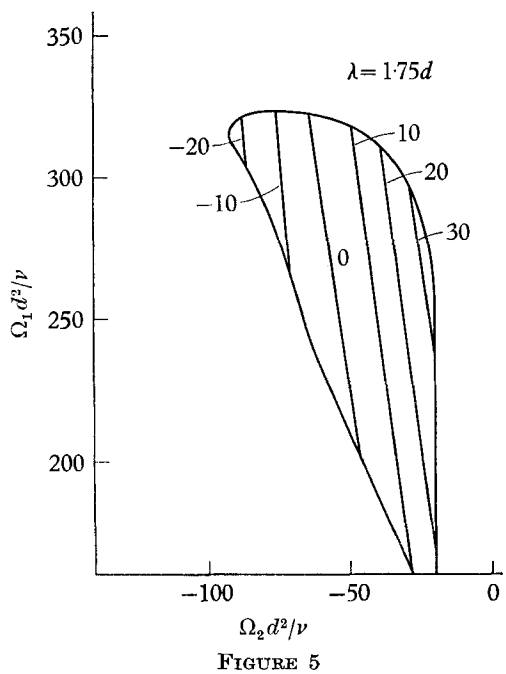

FIGURE 5

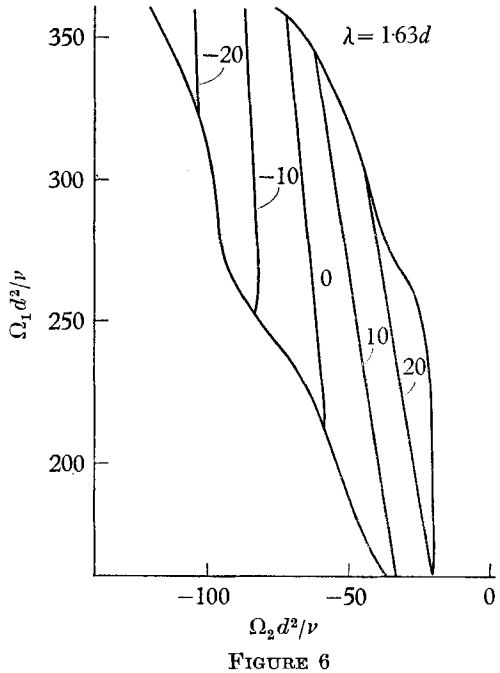

FIGURE 6

FIGURE 5. Contours in the Reynolds number plane of constant dimensionless drift velocity of the wave-form when the wavelength is maintained at 1·75 times the gap width.

FIGURE 6. Contours in the Reynolds number plane of constant dimensionless drift velocity of the wave-form when the wavelength is maintained at 1·63 times the gap width.

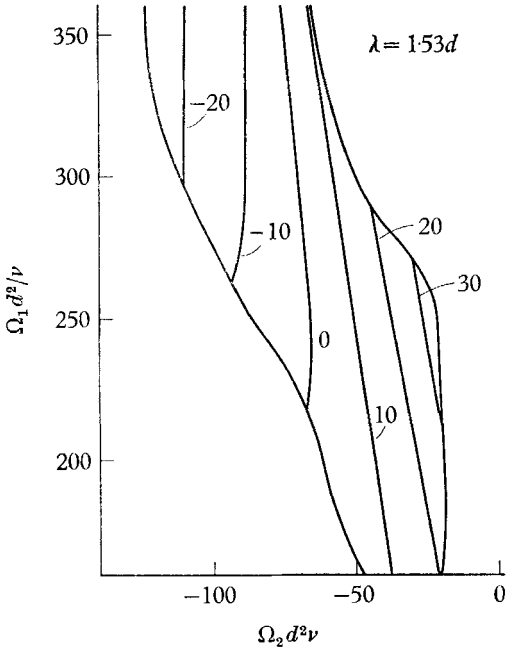

FIGURE 7

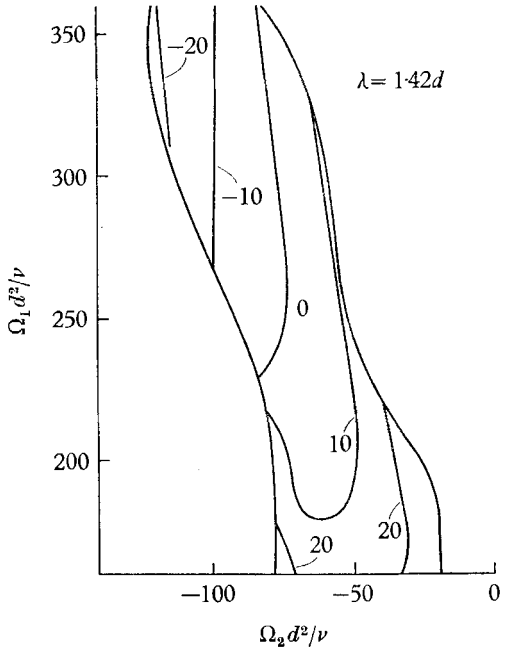

FIGURE 8

FIGURE 7. Contours in the Reynolds number plane of constant dimensionless drift velocity of the wave-form when the wavelength is maintained at 1·53 times the gap width.

FIGURE 8. Contours in the Reynolds number plane of constant dimensionless drift velocity of the wave-form when the wavelength is maintained at 1·42 times the gap width.

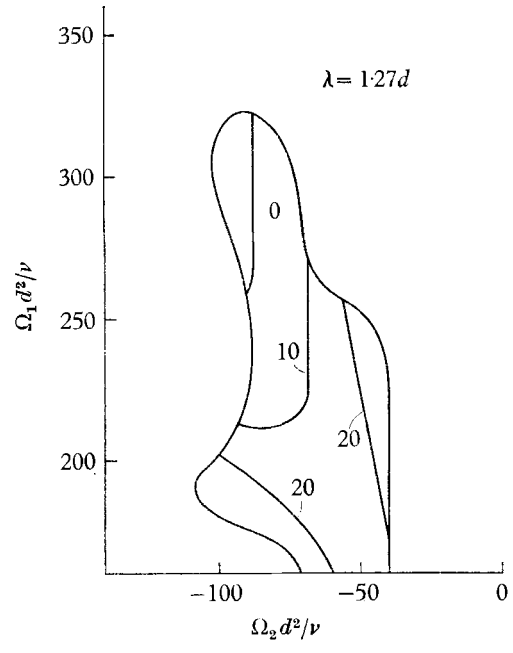

FIGURE 9

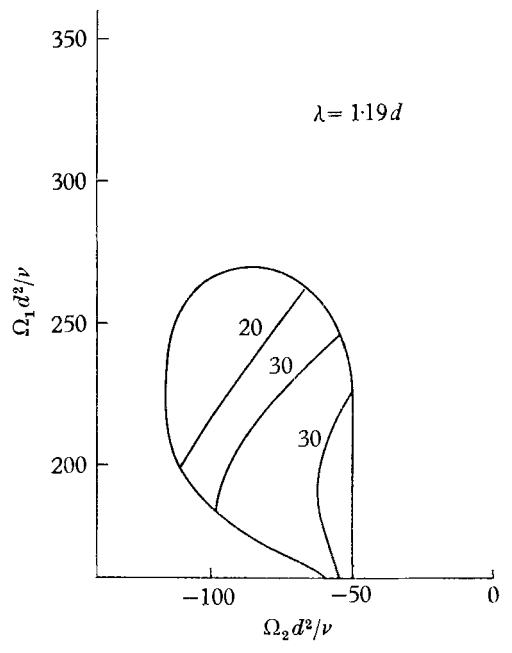

FIGURE 10

FIGURE 9. Contours in the Reynolds number plane of constant dimensionless drift velocity of the wave-form when the wavelength is maintained at 1·27 times the gap width.

FIGURE 10. Contours in the Reynolds number plane of constant dimensionless drift velocity of the wave-form when the wavelength is maintained at 1·19 times the gap width.

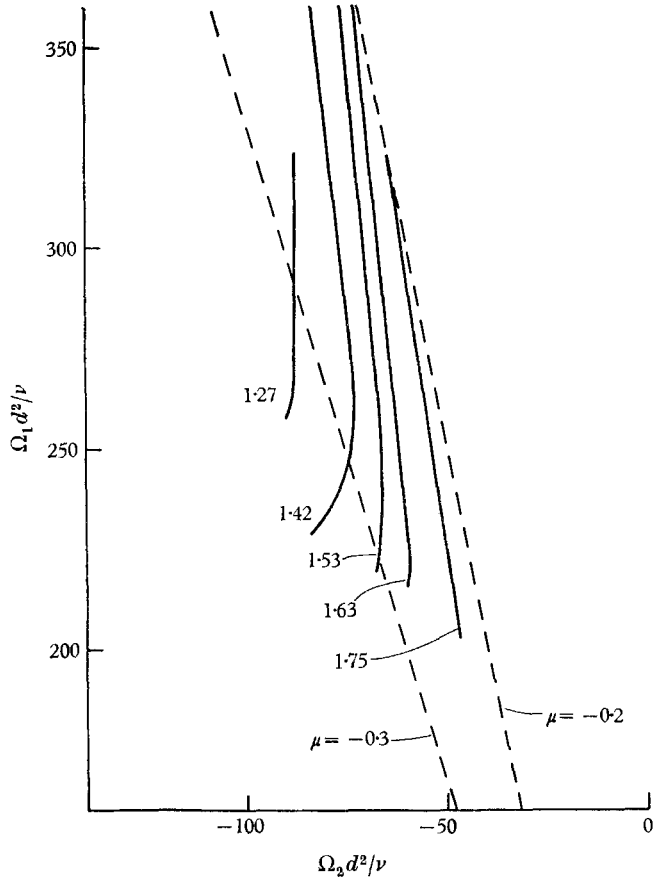

FIGURE 11. Contours in the Reynolds number plane of zero drift velocity of the wave-form in the laboratory frame for different values of the wavelength. The numbers on the contours are the wavelength scaled by the gap width.

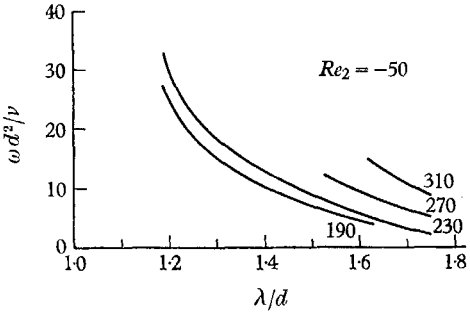

FIGURE 12

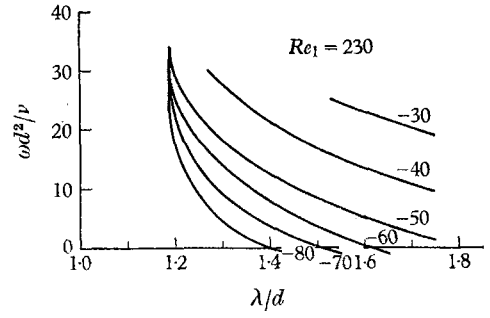

FIGURE 13

FIGURE 12. The dimensionless angular drift velocity of the wave-form $m = 2$ *vs.* the dimensionless wavelength for various values of the Reynolds number of the inner cylinder. The Reynolds number of the outer cylinder is fixed at -50.

FIGURE 13. The dimensionless angular drift velocity of the wave-form $m = 2$ *vs.* the dimensionless wavelength for various values of the Reynolds number of the outer cylinder. The Reynolds number of the inner cylinder is fixed at 230.

constructed. This set of curves shows the extent of the mode $m = 2$ on the three dimensions Re_1, Re_2 and λ/d. The contours are lines of constant dimensionless angular drift velocity $\omega d^2/\nu$. The most significant drift velocity is zero, no drift in the laboratory frame. Figure 11 shows the contours of zero drift velocity for various values of λ/d.

Finally, it is appropriate to show the angular drift velocity *vs.* the wavelength, first at various values of Re_1 and fixed Re_2, and then at various Re_2 for fixed Re_1. The fixed values of Re_1 and Re_2 are picked to be near the centre of the region $m = 2$ shown in figure 1; they are $Re_1 = 230$, $Re_2 = -50$. The results are shown in figures 12 and 13.

4. Discussion

4.1. *On the drift velocity and non-uniqueness*

Most of what we set out to demonstrate can be inferred from figure 3: end effects are not important in the problem of uniqueness if the length to gap ratio is greater than 10; this has been the case for all the data reported by Coles (1965). The correct complete set of parameters to specify the state of the system when the flow is supercritical is Re_1, Re_2, m, η and λ/d. Variation of λ/d with Re_1 and Re_2 held constant has a large effect on the secondary flow. By changing λ/d one property of the wave-form, the angular drift velocity, can be changed from 10 % of the velocity of the inner cylinder, to zero in the laboratory frame, to 10 % of the velocity of the outer cylinder, i.e. in the opposite direction to the mean flow. These variations in the wavelength may be made independently of Re_1 and Re_2.

The large variation in the wave-form at fixed Re_1 and Re_2 caused by changing λ/d is also evident in the set of figures 5 to 10. It is obvious when comparing these figures that no state diagram can be drawn in the two-dimensional Taylor number plane for disturbances which have finite amplitude. The transition curves above the critical curve are a strong function of λ/d. Even for fixed Re_1, Re_2 and λ/d there is hysteresis in the transitions if the rate of changing the boundary conditions is not very slow compared to the rate of rotation. Figure 1 shows the maximum extent of the region $m = 2$ for attainable values of λ/d.

In comparing the present data with the set of transitions tabulated by Coles (1965), it must be borne in mind that the m type modes in an apparatus with $\eta = 0{\cdot}875$ (Coles's value) is quite different from that shown in figure 2. The mixture of normal modes that make up a finite amplitude mode is a strong function of η. Coles finds that for $\eta = 0{\cdot}875$ and $\mu = 0$ (for our data $\mu \neq 0$) all the modes regardless of m or λ/d have the same angular drift velocity, and its value is approximately $\frac{1}{3}\Omega_1$. Notice the contrast between this result and figures 5 to 10. This difference in behaviour is due to a quite different mixture of normal modes in the two cases.

The saturation of the λ/d curve at about 1·2 as shown in figures 12 and 13 indicates a large readjustment of the velocity field to prevent a decrease of λ/d. There is no similar strong reaction at the upper end of the range of λ/d. The same phenomenon is observed for the mode $m = 0$. (See Snyder (1968*a*) for data on the symmetric mode.) For $m = 0$ the curves of λ/d *vs.* Re_1 at $\mu = 0$ are straight parallel

lines for most values of λ/d. But near the lower end of the range, the slope suddenly gets steeper and the curve is no longer a straight line.

4.2. *On the mean flow*

Intuitively one would suspect that there is a simple relation between the mean motion and the azimuthal drift of the disturbance. In fact, it seems reasonable to expect the drift velocity to equal the mean azimuthal velocity. When the linear theory is applied to a wave-form which is a simple normal mode having $m > 0$, and if the unperturbed mean flow is $V = Ar + B/r$, this is actually the calculated result. Accordingly, it appears promising to try to find an analytical expression relating the mean flow, the drift velocity and possibly some averaged functions of the disturbance velocities.

Stuart (1958) has shown how the mean flow at finite amplitude can be calculated from the boundary conditions and from the mean values of velocity component functions associated with the secondary flow. His treatment is restricted to rotationally symmetric flows. An extension of the method to the doubly periodic case is straight forward. The velocity components in circular co-ordinates $(r, \theta, z) \rightarrow (u, v, w)$ are now of the form

$$u = \sum_{n,\, q=0}^{\infty} [U_{nq}(r,t)\exp\{i(nkz+qm\theta)\} + U_{\tilde{n}\tilde{q}}(r,t)\exp\{i(-nkz+qm\theta)\} + U_{n\tilde{q}}(r,t)\exp\{-i(-nkz+qm\theta)\} + U_{\tilde{n}\tilde{q}}(r,t)\exp\{-i(nkz+qm\theta)\}, \quad (1)$$

with similar expressions for $v - V$, w and the pressure p. The functions U_{nq} and $U_{\tilde{n}\tilde{q}}$ are complex conjugates, while U_{nq} and $U_{\tilde{n}q}$ are complex conjugates only with respect to the subscript n. When these expressions are substituted into the Navier–Stokes and continuity equations an infinite sequence of nonlinear equations results. There is a set of equations for each normal mode (n or $\tilde{n}$, q or $\tilde{q}$); the mean motion represents a special case with mode number (0, 0).

It is found that the set of equations associated with (0, 0), i.e. the averaged value equations, are identical to Stuart's mean motion equations. The added complexity of the asymmetric modes does not enter into the determination of the mean flow. Thus, we may write

$$\frac{\partial V}{\partial t} = \frac{1}{r^2}\frac{\partial}{\partial r}(r^2\overline{uv}) = \nu\left(\frac{\partial^2}{\partial r^2} + \frac{1}{r}\frac{\partial}{\partial r} - \frac{1}{r^2}\right)V, \quad (2)$$

following Stuart, and note that

$$\overline{uv} = \sum_{n,\, q=0}^{\infty} [U_{nq}V_{\tilde{n}q} + U_{n\tilde{q}}V_{\tilde{n}q} + U_{\tilde{n}q}V_{n\tilde{q}} + U_{\tilde{n}\tilde{q}}V_{nq}]. \quad (3)$$

It does not appear that the equations, (2) and the related equation for the pressure, may be reformulated in terms of different averages so as to show explicit dependence on ω. The mean equations do not give the desired relationship between ω and V. We also find that when the time dependence $\exp(i\omega t)$ and its complex conjugate are substituted into (2), V is independent of time; the term $\partial V/\partial t$ may be omitted for periodic flows.

The equations generated by equating the coefficients of the higher normal modes all contain ω and V explicitly. However, these equations are extremely difficult to solve. Only two special cases have been investigated, and in both cases the application of the results is limited to the narrow gap geometry. (See Krueger, Gross & DiPrima 1966, and Davey, DiPrima & Stuart 1968.) Extreme truncation of the series (1) has been used in both investigations and therefore the results are limited to small amounts of harmonic generation, i.e. small amplitudes. Even in these simplified examples there is no uncomplicated analytic relation between V and ω.

Another approach to the problem is: (*a*) to start with Stuart's (1958) solution of equation (2) with $\partial V/\partial t = 0$; (*b*) to average the resulting V over the width of the gap obtaining $\overline{V}$; (*c*) to assume a relation between ω and $\overline{V}$; and (*d*) to see if consistent values of the adjustable parameters may be chosen. For $\eta = \frac{1}{2}$ we find

$$\overline{V} = \Omega_1 d(0{\cdot}425 + 1{\cdot}075\mu) - 1{\cdot}075 Z d/\nu + Z^* d/\nu, \tag{4}$$

where $$Z = \int_d^{2d} (\overline{uv}/r)\,dr \quad \text{and} \quad Z^* = (1/d^2)\int_d^{2d} r \int_d^r (\overline{uv}/r')\,dr'\,dr.$$

We need (4) expressed in terms of Re_1 and Re_2; therefore the dependence of Z and Z^* on the Reynolds numbers must be determined. Davey (1962) has analyzed the non-linear stability problem for $\eta = \frac{1}{2}$ when the wave-form is rotationally symmetric and $\mu = 0$; he also treated the case $\eta \to 1$ for $\mu \neq 0$. Following his method we note that to a first approximation $u = A_e u_1' \Omega_1 d/Re_1$ and $v = A_e v_1' \Omega_1 d$, where $A_e^2 = \beta(1 - Re_{1,\mathrm{crit}}^2/Re_1^2) f(\mu)$, and both u_1' and v_1' are independent of the Reynolds numbers but are functions of r, and β is a constant. Thus

$$uv \approx (A_e^2 \Omega_1^2 d^2/Re_1) u_1' v_1',$$

$Zd/\nu = \Omega_1 d A_e^2 Z_0$ and $Z^* d/\nu = \Omega_1 d A_e^2 Z_0^*$, where Z_0 and Z_0^* are pure numbers. For the data in question $Re_1^2 > 5\,Re_{1,\mathrm{crit}}^2$ so that $A_e^2 \approx \beta f(\mu)$. Since $f(\mu) \to 1$ as $\mu \to 0$, we will write $f(\mu) = 1 + C_1\mu + C_2\mu^2 + \ldots$, and thus, to the accuracy of our approximation

$$\overline{V}/\Omega_1 d \approx 0{\cdot}43 + \mu + \beta(Z_0^* - Z_0)(1 + C_1\mu). \tag{5}$$

Assuming the dimensionless drift velocity $R_d = \omega d^2/\nu$ is approximately equal to $\overline{V} d/\nu$ we find that

$$Re_1 \approx \frac{\{R_d - [1 + C_1\beta(Z_0^* - Z_0)]\,Re_2\}}{[0{\cdot}43 + \beta(Z_0^* - Z_0)]} \tag{6}$$

is a first approximation to the data of figures 5 to 11.

Note that by (6) the slope $\partial Re_1/\partial Re_2$ is independent of R_d, Re_1 and Re_2. The data shows nearly constant slope throughout most of the region. Variations in C_1 and $(Z_0^* - Z_0)$ can account for deviations from the average slope. The average value of $\partial Re_1/\partial Re_2$ is observed to be very close to -10. The data also shows that $\partial R_d/\partial Re_2$ is roughly constant at 0·7. Combining these two results with (6) and Davey's value of β (for $\eta = \frac{1}{2}$ and $\mu = 0$) it appears that $C_1 \approx 7{\cdot}5 \times 10^{-2}$ and $(Z_0^* - Z_0) = 40$. Both values are reasonable if we assume that the motion is not vastly different from the case $\mu = 0$ and the same value of Re_1. Using Davey's

u_1' and v_1' we find $(Z_0^* - Z_0) \approx 20$. The narrow gap study of Davey indicates that in that case, the results are not strongly dependent on μ near $\mu = 0$, thus a small value for C_1.

Most of the results are consistent with this crude theory whose main premise is that the drift velocity is close to the mean azimuthal velocity throughout the gap. Equation (6) predicts that for $R_d = 0$, the case shown in figure 11, all curves with the same slope should coincide. It appears that we have to go to a higher order of approximation to account for the variation of ω with λ. We note, however, that except for the cases when λ is near saturation, the different curves are quite close together and they get more so as $Re_1/Re_{1,\text{crit}}$ gets larger.

We could use the slopes $\partial Re_1/\partial Re_2$ and $\partial R_d/\partial Re_2$ from the data to find C_1 and $(Z_0^* - Z_0)$, and thence work back to the amplitude of circulation of the cells and to $\overline{uv}$. But due to the restriction to $u \propto u_1'$ and $v \propto v_1'$, i.e. no appreciable harmonic generation, the theory is not sufficiently precise to give reliable information

In closing we wish to call attention to some other results on this problem which are of a technical nature. The drift velocity is very responsive to changes in viscosity for constant Re_1, Re_2 and λ; the instrument can be used as a viscometer. In exploring the feasibility of using the apparatus for viscosity measurements we investigated the sensitivity of the apparatus to slight imperfections in: centring the shafts; out-of-roundness of the cylinders; tilt of the shafts; small thermal gradients; etc. The interested reader is referred to Snyder (1968*c*).

The hospitality of the Woods Hole Oceanographic Institution during a visit, in the course of which this report was written, is gratefully acknowedged. Funds for the initial work on this project were provided by Contract AF 19(628)-4783 with the Air Force Cambridge Research Laboratories, Office of Aerospace Research. Continued support was received from the National Science Foundation under Grants GK 1007 and GP 6344. The present research is supported by the Office of Naval Research under Contract N00014-66-CO241. It is contribution no. 2076 from the Woods Hole Oceanographic Institution.

REFERENCES

COLES, D. 1965 Transition in circular Couette flow. *J. Fluid Mech.* **21**, 385–425.

DAVEY, A. 1962 The growth of Taylor vortices in flow between rotating cylinders. *J. Fluid Mech.* **14**, 336–68.

DAVEY, A., DIPRIMA, R. C. & STUART, J. T. 1968 On the stability of Taylor vortices. *J. Fluid Mech.* **31**, 17–52.

EKHAUS, W. 1965 *Studies in Non-Linear Stability Theory.* New York: Springer.

HAGERTY, W. W. 1946 Ph.D. dissertation, University of Michigan, Ann Arbor.

KRUEGER, E. R., GROSS, A. G. & DIPRIMA, R. C. 1966 On the relative importance of Taylor-vortex and non-axisymmetric modes in flow between rotating cylinders. *J. Fluid Mech.* **24**, 521–538.

LAMBERT, R. B., SNYDER, H. A. & KARLSSON, S. K. F. 1965 Hot thermistor anemometer for finite amplitude stability measurements. *Rev. Sci. Instr.* **36**, 924–28.

SEGEL, L. A. 1966 Non-linear hydrodynamic stability theory and its application to thermal convection and curved flows. *Non-equilibrium Thermodynamics, Variation Techniques and Stability*, edited by R. J. Donnelly, R. Herman & I. Prigogine. University of Chicago Press.

SNYDER, H. A. 1968*a* Wave-number selection at finite amplitude in rotating Couette flow. *J. Fluid Mech.* **35**, 273.

SNYDER, H. A. 1968*b* Stability of rotating Couette flow. Part I. Asymmetric waveforms. *Phys. Fluids*, **11**, 728.

SNYDER, H. A. 1968*c* A rotating cylinder viscometer. *Rev. Sci. Instr.* (to appear).

SNYDER, H. A. & KARLSSON, S. K. F. 1964 Experiments on the stability of Couette motion with a radial thermal gradient. *Phys. Fluids*, **7**, 1696–1706.

SNYDER, H. A. & LAMBERT, R. B. 1966 Harmonic generation in Taylor vortices between rotating cylinders. *J. Fluid Mech.* **26**, 545–62.

STUART, J. T. 1958 On the non-linear mechanics of hydrodynamic stability. *J. Fluid Mech.* **4**, 1–21.